



**HAL**  
open science

# A formal $\Gamma$ -convergence approach for the detection of points in 2-D images

Daniele Graziani, Laure Blanc-Féraud, Gilles Aubert

► **To cite this version:**

Daniele Graziani, Laure Blanc-Féraud, Gilles Aubert. A formal  $\Gamma$ -convergence approach for the detection of points in 2-D images. [Research Report] RR-7038, INRIA. 2009, pp.25. inria-00418526

**HAL Id: inria-00418526**

**<https://inria.hal.science/inria-00418526>**

Submitted on 19 Sep 2009

**HAL** is a multi-disciplinary open access archive for the deposit and dissemination of scientific research documents, whether they are published or not. The documents may come from teaching and research institutions in France or abroad, or from public or private research centers.

L'archive ouverte pluridisciplinaire **HAL**, est destinée au dépôt et à la diffusion de documents scientifiques de niveau recherche, publiés ou non, émanant des établissements d'enseignement et de recherche français ou étrangers, des laboratoires publics ou privés.

*A formal  $\Gamma$ -convergence approach for the detection  
of points in 2-D images.*

Daniele Graziani, Laure BLANC-FÉRAUD, Gilles Aubert

**N° 7038**

2009

2

Thème COG



*Rapport  
de recherche*



3    **A formal  $\Gamma$ -convergence approach for the detection of**  
4                                   **points in 2-D images.**

5                   Daniele Graziani\*, Laure BLANC-FÉRAUD\*, Gilles Aubert†

6                                   Thème COG — Systèmes cognitifs  
7                                   Projet ARIANA

8                                   Rapport de recherche n° 7038 — 2009 — xxiv pages

9    **Abstract:** We propose a new variational model to isolate points in a 2-dimensional image.  
10 To this purpose we introduce a suitable functional whose minimizers are given by the points  
11 we want to detect. In order to provide numerical experiments we replace this energy with a  
12 sequence of a more treatable functionals by means of the notion of  $\Gamma$ -convergence.

13 **Key-words:** points detection, curvature-depending functionals, divergence-measure fields,  
14  $\Gamma$ -convergence, biological 2-D images.

\* ARIANA Project-team, CNRS/INRIA/UNSA, 2004 Route des lucioles-BP93, 06902 Sophia-Antipolis  
Cedex, France

† LABORATOIRE J.A. DIEUDONNÉ Université de Nice SOPHIA ANTIPOLIS, parc valrose 06108 Nice  
CEDEX 2, FRANCE.

15 A  $\Gamma$ -convergence approach for the detection of points in  
16 2-D images.

17 **Résumé :**

18 **Mots-clés :**

19	<b>Contents</b>	
20	<b>1 Introduction</b>	<b>ii</b>
21	<b>2 Preliminaries</b>	<b>v</b>
22	2.1 Convergence for a set of points . . . . .	v
23	2.2 Distributional divergence . . . . .	v
24	2.3 The Dirichlet problem with measure data . . . . .	vi
25	<b>3 Existence result</b>	<b>vii</b>
26	<b>4 <math>\Gamma</math>-convergence</b>	<b>x</b>
27	4.1 Modica Mortola's approach . . . . .	x
28	4.2 De Giorgi's conjecture . . . . .	x
29	<b>5 The approximating functionals</b>	<b>xii</b>
30	<b>6 Detection</b>	<b>xv</b>
31	6.1 Discretization . . . . .	xv
32	6.2 Discretization in time . . . . .	xvi
33	<b>7 Computer examples</b>	<b>xvii</b>
34	7.1 Parameter settings . . . . .	xvii
35	7.2 Commentaries . . . . .	xvii
36	<b>8 Conclusion</b>	<b>xxii</b>
37	<b>References</b>	<b>xxiii</b>

## 38 1 Introduction

39 Detecting fine structures, like points or curves in two or three dimensional images respec-  
 40 tively, is an important issue in image analysis. In biological images a point may represent  
 41 a viral particle whose visibility is compromised by the presence of other structures like cell  
 42 membranes or some noise.

43 From a variational point of view the problem of isolating points is a difficult task, since it  
 44 is not clear how these singularities must be classified in terms of some differential operator.  
 45 Indeed, since these are usually defined as discontinuity without jump, we cannot use the  
 46 gradient operator as in the classical problem of contours detection. As a consequence the  
 47 functional framework we have to deal with may be not clear.

48 One possible strategy to overcome this obstacle is considering these kinds of pathology  
 49 as a  $k$ -codimension object, meaning that they should be regarded as a singularity of a map  
 50  $U : \mathbb{R}^{k+m} \rightarrow \mathbb{R}^k$ , with  $k \geq 2$  and  $m \geq 0$  (see [7] for a complete survey on this subject). So  
 51 that the detecting point case corresponds to the case  $k = 2$  and  $m = 0$ .

52 In this direction, in [5], the authors have suggested a variational approach based on the  
 53 theory of Ginzburg-Landau systems. In their work the isolated points in 2-D images are  
 54 regarded as the topological singularities of a map  $U : \mathbb{R}^2 \rightarrow \mathbb{S}^1$ , where  $\mathbb{S}^1$  is a unit sphere of  
 55  $\mathbb{R}^2$ . So that it is crucial to construct, starting from the initial image  $I : \mathbb{R}^2 \rightarrow \mathbb{R}$ , an initial  
 56 vector field  $U_0 : \mathbb{R}^2 \rightarrow \mathbb{S}^1$  with a topological singularity of degree 1 at points in the initial  
 57 image  $I$  where the intensity is high. How to do this in a rigorous way, it is a subject of a  
 58 current investigation.

59 Here our purpose is to provide a lighter variational formulation, in which the singularity  
 60 in the image is directly given in terms of a proper differential operator defined on vector  
 61 fields. Another important difference is that in [5] points and curves are detected both as  
 62 singularities, while in the present paper our aim is to isolate from the initial image points  
 63 and at same time remove any other singularities like curves precisely. In our model  $\Omega \subset \mathbb{R}^2$   
 64 is an open set and represents the image domain.

65 In order to detect the singularities of the image, we have to find a functional space  
 66 whose elements generate, in a suitable sense, a measure concentrated on points. Such a  
 67 space is  $\mathcal{DM}^p(\Omega)$  introduced in [4] where  $1 < p < 2$ , the space of vector fields  $U : \Omega \rightarrow \mathbb{R}^2$   
 68 whose distributional divergence is a Radon measure (see Subsection 2.2 for definitions and  
 69 examples). The restriction  $1 < p < 2$  is due to the initialization (see subsection 2.3).

70 Unfortunately even if we are capable of constructing an initial vector field  $U_0$  (see below  
 71 for such a construction) belonging to the space  $\mathcal{DM}^p(\Omega)$ , its singular set could contains  
 72 several structures we want to remove from the original image like for instance curve or some  
 73 noise. Hence, after the initialization we have to clear away all the structures we are not  
 74 interested in by building up, starting from the initial data  $U_0$ , a new vector field  $U$  whose  
 75 singularities are given by the points of the image  $I$  we want to isolate.

76 Thus, from one hand we have to force the concentration set of the distributional diver-  
 77 gence of  $U_0$  to contain only the points we want to catch, and on the other hand we have  
 78 to regularize the initial data  $U_0$  outside the points of singularities. To this end we propose  
 79 to minimize an energy involving a competition between a divergence term and the counting

80 Hausdorff measure  $\mathcal{H}^0$ . More precisely the energy is the following

$$\int_{\Omega \setminus P} |\operatorname{div} U|^2 + \lambda \int_{\Omega} |U - U_0|^p + \mathcal{H}^0(P). \quad (1)$$

81 where  $U \in L^{p,2}(\operatorname{div}; \Omega \setminus P)$  is the space of  $L^p$ -vector fields whose distributional divergence  
 82 belongs to  $L^2(\Omega \setminus P)$ ,  $P$  is the atomic set we want to target and  $\lambda$  is a positive weight. The  
 83 first integral forces  $U$  to be regular outside  $P$ , while the term  $\mathcal{H}^0(P)$  penalizes the presence  
 84 of singular curves in the image.

85 From a practical point of view, this choice allows us to work with a first order differential  
 86 operator and permits us to formulate the minimization problem in a common functional  
 87 framework.

88 Clearly for initializing the minimization process we need to construct from the initial  
 89 image, a vector field  $U_0$  belonging to  $\mathcal{DM}^p(\Omega)$ . Such a vector field can be provided by the  
 90 gradient of weak solution of the classical Dirichlet problem with measure data.

$$\begin{cases} \Delta f = I & \text{on } \Omega \\ f = 0 & \text{on } \partial\Omega. \end{cases} \quad (2)$$

91 In order to provide computer examples, we must approximate functional (1) by means of a  
 92 sequence of more convenient functionals.

93 The approximation, we suggest in this paper, is based on the so called  $\Gamma$ -convergence,  
 94 the notion of variational convergence introduced by De Giorgi (see [13, 14]). This theory  
 95 is designed to approximate a variational problem by a sequence of different variational  
 96 problems. The most important feature of the  $\Gamma$ -convergence relies on the fact that it implies  
 97 the convergence of minimizers of the approximating functionals to those of the limiting  
 98 functional. In this work we suggest a possible  $\Gamma$ -convergence approach for the detection of  
 99 points. By the way we stress out that the  $\Gamma$  convergence result is only conjectured in this  
 100 paper, whose purpose is to test a new variational method from an experimental point of  
 101 view. For a rigorous variational approximation in a particular case, we refer the reader to  
 102 [6].

103 Classically variational approximation techniques such as  $\Gamma$ -convergence or continuation  
 104 method (see [2, 3] and [20] respectively) have been successfully employed in image and signal  
 105 processing.

106 For instance in ([2, 3]) Ambrosio and Tortorelli have proven that the classical Mumford-  
 107 Shah's functional for detecting 1-dimensional smooth boundaries, can be approximated by  
 108 a sequence of elliptic functionals that are numerically more treatable.

The main difficulty here is related to the presence of a codimension 2 object, which is not  
 a contour: the set  $P$ . In order to obtain a variational approximation close to the one provided  
 in ([2, 3]), the crucial step is then to replace the term  $\mathcal{H}^0(P)$  of functional (1) by a more  
 handy, from a variational point of view, functional involving a smooth boundary and his  
 perimeter given by the 1-dimensional Hausdorff measure  $\mathcal{H}^1$ . Following some suggestion from  
 the paper of Braides and Malchiodi and Braides and March (see [9, 10]) such a functional



is given by:

$$G_{\beta_\varepsilon}(D) = \frac{1}{4\pi} \int_{\partial D} \left( \frac{1}{\beta_\varepsilon} + \beta_\varepsilon \kappa^2(x) \right) d\mathcal{H}^1(x),$$

109 where  $D$  is a proper regular set containing the atomic set  $P$ ,  $\kappa$  is the curvature of its  
110 boundary, the constant  $\frac{1}{4\pi}$  is a normalization factor, and  $\beta_\varepsilon$  infinitesimal as  $\varepsilon \rightarrow 0$ . Roughly  
111 speaking the minima of this functional are achieved on the union of balls of small radius, so  
112 that when  $\beta_\varepsilon \rightarrow 0$  the functional shrinks to the atomic measure  $\mathcal{H}^0(P)$ . On the other hand  
113 the introduction of a curvature term requires a non trivial and convenient, for a numerical  
114 point of view, approximation of the curvature-dependent functional. Such an approximation  
115 is based on a celebrated conjecture due to De Giorgi (see [12]). By means of this argument  
116 it is possible to substitute the curvature-depending functional with an integral functional  
117 involving the Laplacian operator of smooth functions. Then it remains to approximate  
118 the  $\mathcal{H}^1$ -measure and this can be done by retrieving a classical gradient approach used in  
119 [15, 16]. This strategy allows to deal with a functional whose Euler-Lagrange equations  
120 can be discretized. A simple and intuitive explanation of the construction of the complete  
121 approximating functionals will be given in section 3.

122 The paper is organized as follows: section 2 is intended to remind the reader of math-  
123 ematical tools useful in the following. In section 3 we address the existence result for the  
124 functional  $F(U, P)$  defined in (1). In section 4 we state the two well-known  $\Gamma$ -convergence  
125 results we need in the sequel. In section 5 we build in a formal way the approximating  
126 sequence. In section 6 we present the discrete model and the detection strategy. Finally the  
127 last section is devoted to some computer examples.

## 128 2 Preliminaries

### 129 2.1 Convergence for a set of points

130 For our purpose it will be crucial dealing with a notion of convergence for finite sets of points  
131 introduced in [10].

132 **Definition 2.1.** We say that a sequence of a finite set of points  $\{P_h\} \subset \overline{\Omega}$  converges to  
133 a set  $P \subset \overline{\Omega}$  if each of the sets  $P_h$  contains a number  $N$  of points  $\{x_h^1, \dots, x_h^N\}$ , with  $N$   
134 independent of  $h$ , such that  $x_h^i \rightarrow x^i$  for any  $i = 1, \dots, n$  and  $\bigcup_{i=1}^N \{x_i\} = P$ .

135 **Lemma 2.1.** Let  $\{P_h\}$  be a sequence of a finite set of points such that  $\mathcal{H}^0(P_h) \leq N_0$  for  
136 every  $h$  with  $N_0 \in \mathbb{N}$ . Then there exists a subsequence  $\{P_{h_k}\} \subset \{P_h\}$  and a set of points  
137  $P \subset \overline{\Omega}$  such that  $P_{h_k}$  converges with respect to the convergence 2.1 to the set  $P$ .

138 **Proof.** Since  $\mathcal{H}^0(P_h) \leq N_0$ , we may find  $N_1 \leq N_0$  such that every set  $P_h$  contains  $N_1$  points.  
139 For every  $i = 1, \dots, N_1$  and there exists a subsequence  $x_{h_k}^i \subset x_h^i$  converging to  $x^i \in \overline{\Omega}$ .

140 Then by setting  $P_{h_k} = \bigcup_{i=1}^{N_1} x_{h_k}^i$  and  $P = \bigcup_{i=1}^{N_1} x^i$ , the thesis is achieved.

141 **Lemma 2.2.** Let  $\{P_h\} \subset \overline{\Omega}$  be a sequence of finite set of points converging to a finite set of  
142 points  $P$ . Then

$$\mathcal{H}^0(P) \leq \liminf_{h \rightarrow +\infty} \mathcal{H}^0(P_h) \quad (3)$$

**Proof.** From definition 2.1 it follows that

$$\liminf_{h \rightarrow +\infty} \mathcal{H}^0(P_h) \geq \liminf_{h \rightarrow +\infty} H^0(\{x_h^1, \dots, x_h^N\}) = N = \mathcal{H}^0(P). \quad \square$$

### 143 2.2 Distributional divergence

144 In this subsection we recall the definition of the space  $L^{p,q}(\text{div}; \Omega)$  and  $\mathcal{DM}^p(\Omega)$ , introduced  
145 in [4].

146 Let  $\Omega \subset \mathbb{R}^2$  be an open set and let  $U : \Omega \subset \mathbb{R}^2 \rightarrow \mathbb{R}^2$  be a vector field.

147 **Definition 2.2.** We say that  $U \in L^{p,q}(\text{div}; \Omega)$  if  $U \in L^p(\Omega; \mathbb{R}^2)$  and if its distributional  
148 divergence  $\text{div}U \in L^q(\Omega)$ . If  $p = q$  the space  $L^{p,q}(\text{div}; \Omega)$  will be denoted by  $L^p(\text{div}; \Omega)$ .

149 We say that  $U \in L_{loc}^{p,q}(\text{div}; \Omega)$  if  $U \in L^{p,q}(\text{div}; A)$  for every open set  $A \subset\subset \Omega$ .

**Definition 2.3.** For  $U \in L^p(\Omega; \mathbb{R}^2)$ ,  $1 \leq p \leq +\infty$ , set

$$|\text{div}U|(\Omega) := \sup \left\{ \int_{\Omega} U \cdot \nabla \varphi dx dy : \varphi \in C_0^1(\Omega), |\varphi| \leq 1 \right\}.$$

We say that  $U$  is an  $L^p$ -divergence measure field, i.e.  $U \in \mathcal{DM}^p(\Omega)$  if

$$\|U\|_{\mathcal{DM}^p(\Omega)} := \|U\|_{L^p(\Omega; \mathbb{R}^2)} + |\text{div}U|(\Omega) < +\infty.$$

150 We say that  $U \in \mathcal{DM}_{loc}^p(\Omega)$  if  $U \in \mathcal{DM}^p(A)$  for every open set  $A \subset\subset \Omega$ .

151 **Remark 2.1.** If  $U \in \mathcal{DM}^p(\Omega)$  then via Riesz Theorem it is possible to represent the distri-  
 152 butional divergence of  $U$  by a Radon measure. More precisely there exists a Radon measure  
 153  $\mu$  such that for every  $\varphi \in C_0^1(\Omega)$  the following equality holds:

$$\int_{\Omega} U \cdot \nabla \varphi dx dy = - \int_{\Omega} \varphi d\mu.$$

154 For instance the field  $U(x, y) = (\frac{x}{x^2+y^2}, \frac{y}{x^2+y^2})$  belongs to  $\mathcal{DM}_{loc}^1(\mathbb{R}^2)$  and its divergence  
 155 measure is given by  $-2\pi\delta_0$ , where  $\delta_0$  is the Dirac mass.

156 Such a result can be proven by approximation. Let us define the following map:

$$U_{\varepsilon}(x, y) := \begin{cases} U(x, y) & \text{if } |x| \geq \varepsilon \\ (\frac{x}{\varepsilon^2}, \frac{y}{\varepsilon^2}) & \text{if } |x| < \varepsilon. \end{cases}$$

157 It is not difficult to check that  $u_{\varepsilon}$  is Lipschitz-map with divergence given by

158  $\frac{2}{\varepsilon^2} \chi_{B(0, \varepsilon)}$ .

159 Then for every test function  $\varphi \in C_0^1(\mathbb{R}^2)$  we have

$$\int U_{\varepsilon} \cdot \nabla \varphi dx dy = - \int \frac{2}{\varepsilon^2} \chi_{B(0, \varepsilon)} \varphi dx dy.$$

By applying the change of variables  $x = \frac{x_1}{\varepsilon}$ ,  $y = \frac{y_1}{\varepsilon}$  we obtain

$$\int U_{\varepsilon} \cdot \nabla \varphi dx dy = -2 \int \chi_{B(0, 1)} \varphi(\frac{x_1}{\varepsilon}, \frac{y_1}{\varepsilon}) dx_1 dy_1,$$

so that, letting  $\varepsilon \rightarrow 0$ , by the dominated convergence theorem we obtain

$$\int_{\Omega} U \cdot \nabla \varphi dx dy = -2\pi \varphi(0, 0) = -2\pi \int_{\Omega} \varphi d\delta_0$$

### 160 2.3 The Dirichlet problem with measure data

161 For the initialization of our algorithm we must build a vector field  $U_0$  which should be such  
 162 that its divergence is singular on points of the image  $I$ . Therefore we will use the gradient  
 163 of the solution of the following Dirichlet problem (applied with  $\mu = I$ )

$$\begin{cases} \Delta f = \mu & \text{on } \Omega \\ f = 0 & \text{on } \partial\Omega \end{cases} \quad (4)$$

164 where  $\mu$  is a Radon measure.

165 Classical results (see [19]) guarantee the existence of a unique solution of problem (4).

166 Concerning the regularity it is known then  $f \in W^{1,p}(\Omega)$  with  $p < 2$ .

### 167 3 Existence result

168 In this section we show the existence of a minimizing pair  $(U, P)$  for the functional  $F$  defined  
 169 in (1.)

170 Our argument needs two steps (see also [17] for a similar approach to minimize the  
 171 classical Mumford-Shah's functional). The first one consists in proving the existence a  
 172 minimizer of the functional (1) when the set  $P$  is fixed.

173 To this aim we adopte the following notation:

174

$$F(U) = F(\cdot, P) = \int_{\Omega \setminus P} |\operatorname{div} U|^2 dx dy + \lambda \int_{\Omega} |U - U_0|^p dx dy + \mathcal{H}^0(P). \quad (5)$$

175 **Theorem 3.1.** *For every set  $P$  there exists a unique minimizer  $U_P \in L^{p,2}(\Omega \setminus P; \operatorname{div})$  of*  
 176 *the functional (5).*

177 **Proof.** Let  $U_n$  be a minimizing sequence. Then we have the following bound

$$F(U_n) \leq M. \quad (6)$$

From the bound (6) and the classical inequality:

$$\|U_n\|_{L^p(\Omega \setminus P)}^p \leq 2^p \|U_n - U_0\|_{L^p(\Omega \setminus P)}^p + \|U_0\|_{L^p(\Omega \setminus P)}^p$$

it follows that

$$\|U_n\|_{L^p(\Omega \setminus P)}^p \leq M + \|U_0\|_{L^p(\Omega \setminus P)}^p := C.$$

Moreoveor we also have:

$$\|\operatorname{div} U_n\|_{L^2(\Omega \setminus P)}^2 \leq F(U_n) \leq M;$$

178 so that, up to subsequences, we obtain

$$\begin{cases} U_n \rightharpoonup U_P & \text{in } L^p(\Omega \setminus P) \\ \operatorname{div} U_n \rightharpoonup \operatorname{div} U_P & \text{in } L^2(\Omega \setminus P). \end{cases} \quad (7)$$

179 Therefore we can conclude that  $U_n$  weakly converges in  $L^{p,2}(\Omega \setminus P; \operatorname{div})$  to a vector field  
 180  $U_P \in L^{p,2}(\Omega \setminus P; \operatorname{div})$ .

Then we have thanks to semicontinuity properties of the  $L^p$ -norm with respect to the weak convergence:

$$\inf_U F(U) \leq F(U_P) \leq \liminf_{n \rightarrow +\infty} F(U_n) = \inf_U F(U).$$

181 Finally the strong convexity of functional (5) gives the uniqueness of the minimizer  $U$   $\square$

182 Once we obtained the existence of the minimizer  $U_P$  for every set  $P$  fixed, we focus on  
 183 the following functional.

184

$$E(P) := F(U_P, P) = \int_{\Omega \setminus P} |\operatorname{div} U_P|^2 dx dy + \lambda \int_{\Omega} |U_P - U_0|^p dx dy + \mathcal{H}^0(P). \quad (8)$$

185 We extend  $U$  and  $\operatorname{div}U$  by zero on  $P$ . However we keep the integration domain of  $\operatorname{div}U$  to  
 186 be  $\Omega \setminus P$ . We do that in order to make clear that  $\operatorname{div}U$  is the distributional divergence of  $U$   
 187 on  $\Omega \setminus P$  and not on  $\Omega$ .

188 The following semicontinuity lemma plays a key role.

**Lemma 3.1.** *Assume that a sequence of finite sets of points  $\{P_n\} \subset \overline{\Omega}$  converges to a finite set of point  $P \subset \overline{\Omega}$ . Then*

$$E(P) \leq \liminf_{h \rightarrow \infty} E(P_n)$$

**Proof.** Let us set  $U_n = U_{P_n}$ , we can assume that  $U_n$  and  $\operatorname{div}U_n$  are both defined on all of  $\Omega$  in the sense explained above. The sequence  $U_n$  is bounded in  $L^p(\Omega)$ . Indeed, by taking into account that  $U_n$  is a minimizer of the functional (5),

$$\|U_n\|_{L^p(\Omega)}^p \leq 2^p \|U_n - U_0\|_{L^p(\Omega)}^p + \|U_0\|_{L^p(\Omega)}^p \leq 2^p F(0) + \|U_0\|_{L^p(\Omega)}^p = \|U_0\|_{L^p(\Omega)}^p (2^p + 1).$$

189 In the same way one can show that the sequence  $\operatorname{div}U_n$  is bounded in  $L^2(\Omega)$ . So that, up to  
 190 subsequences, we may assume

$$\begin{cases} U_n \rightharpoonup U & \text{in } L^p(\Omega) \\ \operatorname{div}U_n \rightharpoonup V & \text{in } L^2(\Omega). \end{cases} \quad (9)$$

We claim that  $\operatorname{div}U = V$  in  $\Omega \setminus P$ . In fact, take any test function  $\varphi$  with support in  $\Omega \setminus P$ , then since  $P_n \rightarrow P$ , we have for  $n$  large enough

$$\operatorname{supp}(\varphi) \subset \Omega \setminus P_n$$

and, consequently,

$$\int_{\operatorname{supp}(\varphi)} U_n \nabla \varphi dx = - \int_{\operatorname{supp}(\varphi)} \operatorname{div}U_n \varphi dx.$$

Therefore, by taking the weak limit by (9) we get

$$\int_{\operatorname{supp}(\varphi)} U \nabla \varphi dx = - \int_{\operatorname{supp}(\varphi)} V \varphi dx.$$

191 Then since the test function  $\varphi$  is arbitrary, we can conclude that  $\operatorname{div}U = V$  on  $\Omega \setminus P$ .  
 The thesis follows because, from the lower semicontinuity of the  $L^p$ -norm and Lemma  
 2.2

$$E(P) \leq E(U, P) \leq \liminf_n E(U_n, P_n) \quad \square$$

192 We are now in position of proving the main result of this section.

193 **Theorem 3.2.** *There exist a minimizer  $(U, P)$  of the functional  $F$ , with  $U \in L^{p,2}(\operatorname{div}; \Omega)$   
 194 and  $P \subset \Omega$  a finite set of points.*

195 **Proof.** For every  $P$  let  $U_P$  a minimizer for the functional  $F$ , whose existence is guaranteed  
 196 by Theorem 3.1

Then we focus on the the functional  $E(P) = F(U_P, P)$  and we take a minimizing sequence  $\{P_n\}$ . Then by Lemma 2.1 we have (up to a subsequences) that  $P_n \rightarrow \bar{P} \subset \bar{\Omega}$  and  $U_{P_n} \rightarrow U_{\bar{P}}$ . By Lemma 3.1 we get

$$E(\bar{P}) \leq \liminf_{n \rightarrow +\infty} E(P_n).$$

197 Therefore

$$\inf_{(U,P)} F(U, P) \leq F(U_{\bar{P}}, \bar{P}) \leq \liminf_{n \rightarrow +\infty} E(P_n) \leq \liminf_{h \rightarrow +\infty} F(U_h, P_h) = \inf_P F(U_P, P) \leq F(U, P), \quad (10)$$

Now set  $\tilde{P} := \bar{P} \setminus \partial\Omega$ . Since for every  $P$ ,  $U_P$  is a minimizer we get from (10)

$$F(U_{\bar{P}}, \tilde{P}) \leq F(U_{\bar{P}}, \bar{P}) \leq F(U_P, P) \leq F(U, P),$$

for every  $(U, P)$ . Hence we conclude that

$$F(U_{\bar{P}}, \tilde{P}) \leq \inf_{(U,P)} F(U, P). \quad \square$$

## 198 4 $\Gamma$ -convergence

199 The key point of our strategy is to replace the functional (1) by means of more regular  
200 functionals by following a formal  $\Gamma$ -convergence approach.

201 Therefore this section is devoted to a very simple presentation of the two results we need:  
202 Modica-Mortola's theorem (see [15, 16]) concerning the approximation of the perimeter and  
203 De Giorgi's conjecture (see [12]) about the approximation of curvature depending function-  
204 als. For the definition of the  $\Gamma$ -convergence and its main properties we refer the reader to  
205 [8, 11] and references therein.

### 206 4.1 Modica Mortola's approach

207 Modica-Mortola theorem states that it is possible to approximate, in the  $\Gamma$ -convergence  
208 sense, a perimeter by means of the following sequence of functionals

$$F_\varepsilon^1(u) := \begin{cases} \int_\Omega (\varepsilon |\nabla u|^2 + \frac{V(u)}{\varepsilon}) dx & \text{if } u \in W^{1,2}(\Omega), \\ +\infty & \text{otherwise,} \end{cases}$$

209 where  $V(u) = u^2(1-u)^2$  is a double well potential. Besides, since the minimizers of the  
210 functional  $F_\varepsilon^1$  may be trivial, some constraint on the functions  $u_\varepsilon$  must be added. Usually  
211 a volume constraint of the type  $\int_\Omega u dx dy = m$ , is assumed.

212 Let us give an intuitive explanation of such a result. Since  $V$  has two absolute minimizers  
213 at  $u = 0, 1$ , when  $\varepsilon$  is small, a local minimizer  $u_\varepsilon$  is close to 1 on a part of  $\Omega$  and close to  
214 0 on the other part, making a rapid transition of order  $\varepsilon$  between 0 and 1. When  $\varepsilon \rightarrow 0$  the  
215 transition set shrinks to a set of dimension 1, so that  $u_\varepsilon$  goes to a function taking values  $u$   
216 into  $\{0, 1\}$  and the family of functionals  $\Gamma$ -converges to the measure of the perimeter of the  
217 discontinuity set of  $u$ . Modica-Mortola's Theorem is the following.

218 **Theorem 4.1.** *The functionals  $F_\varepsilon^1 : L^1(\Omega) \rightarrow [0, +\infty]$   $\Gamma$ -converge with respect to the*  
219  *$L^1$ -convergence to the following functional*

$$F^1(u) = \begin{cases} C_V \mathcal{H}^1(S_u) & \text{if } u \in \{0, 1\} \\ +\infty & \text{otherwise} \end{cases}$$

220 where, as usual,  $S_u$  denotes the set of discontinuities of  $u$  and  $C_V$  is a suitable constant  
221 depending on the potential  $V$ .

### 222 4.2 De Giorgi's conjecture

The aim of De Giorgi was finding a variational approximation of a curvature depending  
functional of the type:

$$F^2(D) = \int_{\partial D} (1 + \kappa^2) d\mathcal{H}^1;$$

223 where  $D$  is a regular set and  $k$  is a curvature of its boundary  $\partial D$ .

224 Since  $\partial D$  can be represented as the discontinuity set of the function  $u_0 = 1 - \chi_D$ ,  
 225 by Modica-Mortola's Theorem it follows that there is a sequence of non constant local  
 226 minimizers such that  $u_\varepsilon \rightarrow u_0$  with respect to the  $L^1$ -convergence such that

$$\lim_{\varepsilon \rightarrow 0} F_\varepsilon^1(u_\varepsilon) := C_V \mathcal{H}^1(\partial D).$$

227 Furthermore looking at the Euler-Lagrange equation associated to a contour length term,  
 228 yields a contour curvature term  $\kappa$ , while the Euler-Lagrange equations for the functional  
 229  $F_\varepsilon^1(u)$  contains a term  $2\varepsilon\Delta u - \frac{V'(u)}{\varepsilon}$ .

230 Then De Giorgi suggested to approximate the functional  $F^2$  by adding to Modica-  
 231 Mortola's approximating functionals the term

$$F_\varepsilon^2(u) = \int_{\Omega} (2\varepsilon\Delta u - \frac{V'(u)}{\varepsilon})^2 (\varepsilon|\nabla u|^2 + \frac{V(u)}{\varepsilon}) dx.$$

In [18] the authors have proven a simplified version of the De Giorgi's conjecture, where the integral above is replaced by the functional

$$F_\varepsilon^2(u) = \int_{\Omega} (2\varepsilon\Delta u - \frac{V'(u)}{\varepsilon})^2 dx.$$



## 232 5 The approximating functionals

233 In this section we present the energy we deal with and the construction of the approximating  
234 sequence.

The energy we are interested in is given by

$$\int_{\Omega \setminus P} |\operatorname{div} U|^2 + \lambda \int_{\Omega} |U - U_0|^p + \mathcal{H}^0(P).$$

235 where  $U \in L^{p,2}(\operatorname{div}; \Omega \setminus P)$ ,  $U_0 \in \mathcal{DM}_{loc}^p(\mathbb{R}^2)$  and finally  $P$  is an atomic set consisting of a  
236 finite number  $N$  of points, i.e.  $P = \{x_1, \dots, x_N\}$ .

As pointed out in the introduction, the first step is to substitute the counting measure  $\mathcal{H}^0(P)$  with a more treatable term given by:

$$G_{\beta_\varepsilon}(D) = \frac{1}{4\pi} \int_{\partial D} \left( \frac{1}{\beta_\varepsilon} + \beta_\varepsilon \kappa^2(x) \right) d\mathcal{H}^1(x);$$

237 where  $D$  is an union of regular simply connected sets  $\{D_i\}$  with  $i = 1, \dots, N$ , such that  
238  $x_i \in D_i$ ,  $D_i \cap D_j = \emptyset$  for  $i \neq j$ .  $\kappa$  is the curvature of the boundary of the set  $D$ , the  
239 constant  $\frac{1}{4\pi}$  is a normalization factor and  $\beta_\varepsilon$  is infinitesimal as  $\varepsilon \rightarrow 0$ .

240 To understand why we can approximate  $\mathcal{H}^0(P)$  with  $G_{\beta_\varepsilon}(D)$  one should note that the  
241 solution of the following minimum problem

$$\min_{D \supset P} G_{\beta_\varepsilon}(D) \tag{11}$$

242 is given by  $D = \bigcup_i^N B(x_i, \beta_\varepsilon)$ , where  $x_i$  are the points of  $P$ . We give an idea of a possible  
243 proof in the case of a single point.

By the Young's inequality we have

$$G_{\beta_\varepsilon}(D) \geq \frac{1}{4\pi} \int_{\partial D} 2\kappa d\mathcal{H}^1(x)$$

244 and by applying the Gauss-Bonnet Theorem

$$G_{\beta_\varepsilon}(D) \geq \frac{1}{4\pi} (2)(2\pi) = 1 = \mathcal{H}^0(P).$$

245 Finally a simple calculation shows that, if we evaluate the functional  $G_{\beta_\varepsilon}$  on  $B(x_1, \beta_\varepsilon)$ ,  
246 we obtain the value 1, i.e. the number of points in  $P$ , i.e.  $\mathcal{H}^0(P)$ . The  $N$  points case can  
247 be recovered with minor changes by the same argument.

For what follows it is convenient to split the functional  $G_{\beta_\varepsilon}$  in two terms:

$$G_{\beta_\varepsilon}(D) = G_{\beta_\varepsilon}^1(D) + G_{\beta_\varepsilon}^2(D)$$

248 where

$$G_{\beta_\varepsilon}^1(D) = \frac{1}{4\pi} \int_{\partial D} \frac{1}{\beta_\varepsilon} d\mathcal{H}^1(x);$$

249 and

$$G_{\beta_\varepsilon}^2(D) := \frac{1}{4\pi} \int_{\partial D} \beta_\varepsilon \kappa^2(x) d\mathcal{H}^1(x).$$

250 We can write an intermediate approximation of energy (1):

$$E_\varepsilon(U, D) = G_{\beta_\varepsilon}^1(D) + G_{\beta_\varepsilon}^2(D) + \int_{\Omega} (1 - \chi_D) |\operatorname{div}(U)|^2 + \lambda \int_{\Omega} |U - U_0|^p. \quad (12)$$

251 The advantage of such a formulation is that we know how to provide a variational ap-  
 252 proximation of the perimeter measure  $H^1 \llcorner \partial D$ . Following Modica-Mortola's approach such  
 253 an approximation can be obtained by using the following measure:

$$\mu_\varepsilon(w, \nabla w) dx = (\varepsilon |\nabla w|^2 + \frac{V(w)}{\varepsilon}) dx,$$

254 where  $V(w) = w^2(1-w)^2$  is a double well functional.

255 Next step is expressing the curvature term by means of the function  $w$ . Thanks to  
 256 the simplified version of the De Giorgi's conjecture we can replace the term  $\kappa$  by the term  
 257  $2\varepsilon \Delta w - \frac{V'(w)}{\varepsilon}$ .

So that we can formally write the complete approximating functional:

$$\begin{aligned} \Phi_\varepsilon(U, w) : &= \int_{\Omega} w^2 |\operatorname{div}(U)|^2 dx + \frac{1}{4\pi} \int_{\Omega} \beta_\varepsilon (2\varepsilon \Delta w - \frac{V'(w)}{\varepsilon})^2 dx + \frac{1}{\beta_\varepsilon} \int_{\Omega} \mu_\varepsilon(w, \nabla w) dx \\ &+ \lambda \int_{\Omega} |U - U_0|^p dx + \frac{2}{\mu_\varepsilon} \int_{\Omega} (1-w)^2 dx, \end{aligned} \quad (13)$$

258 where  $U \in L^{p,2}(\operatorname{div}; \Omega)$  is equal to 0 on the  $\partial\Omega$  and  $w$  is smooth function equal to 1  
 259 on the boundary, i.e.  $1-w \in C_0^\infty(\Omega)$ ,  $\mu_\varepsilon \rightarrow 0$  when  $\varepsilon$  goes to 0. The last integral is a  
 260 penalization term which prevents  $w_\varepsilon$  from converging to the function constantly equal to 0  
 261 as  $\varepsilon \rightarrow 0$ .

262 Then if  $(U_\varepsilon, w_\varepsilon)$  is a minimizing sequence of  $\Phi_\varepsilon$ , then  $w_\varepsilon$  must be very close to the values  
 263 1 when  $\varepsilon$  goes to 0, since the double well potential is positive except for  $w_\varepsilon = 0, 1$  and  $w$   
 264 must be equal to 1 on  $\partial\Omega$ . On the other hand, near the points where the divergence is very  
 265 big  $w_\varepsilon$  must be close to 0. Besides when  $\varepsilon \rightarrow 0$ ,  $\beta_\varepsilon \rightarrow 0$  goes to 0 as well, so that the singular  
 266 set  $D$  is given by an union of balls of a small radius  $\beta_\varepsilon$ .

267 Therefore, while the functions  $U_\varepsilon$  approximate a minimizer  $U$  of the original functional,  
 268 the level set  $\{w_\varepsilon = 0\}$  approximate the original singular set  $P$ .

269 **Remark 5.1.** We point out that the  $\Gamma$ -convergence result is not proved in this paper, but  
 270 only conjectured. A complete proof of the  $\Gamma$ -convergence result and the equicoerciveness of the  
 271 sequence  $\Phi_\varepsilon$ , in the particular case where the vector field  $U$  is a gradient, has been provided  
 272 by the first and third author in [6].

The first variation of this functional leads to the following gradient flow system

$$\begin{aligned}\frac{\partial U}{\partial t} &= 2\nabla(w^2 \operatorname{div} U) + \lambda p |U - U_0|^{p-2} (U - U_0) \\ \frac{\partial w}{\partial t} &= -4 \frac{\Delta h}{\beta_\varepsilon} + \beta_\varepsilon h + \frac{2}{\varepsilon^2} \frac{1}{\beta_\varepsilon} V''(w) h - 2w |\operatorname{div} U|^2 + 2 \frac{1}{\mu_\varepsilon} (1 - w),\end{aligned}\quad (14)$$

273 where  $h$  is given by the equation

$$h = 2\varepsilon \Delta w - \frac{1}{\varepsilon} V'(w).$$

## 274 6 Detection

275 In our model the image contains an atomic Radon measure. Thus, in order to find an initial  
 276 vector field which copies the singularities of the initial image, we use the gradient of the  
 277 solution of the following Dirichlet problem:

$$\begin{cases} \Delta f = I & \text{on } \Omega \\ f = 0 & \text{on } \partial\Omega. \end{cases} \quad (15)$$

278 In this way we obtain a vector field whose divergence is singular on a proper set which  
 279 contains the points we want to detect. In general this set could contain other structures.  
 280 For instance if the initial image is a Radon measure concentrated both on points and on  
 281 curves, the divergence of  $\nabla f$  is singular on points and on curves at the same time. Besides  
 282 if there is some noise in the image, it could be not clear how to differentiate the singular  
 283 points due to the noise, from those we want to catch. As a consequence, by solving problem  
 284 (15), we get just a predetection, which has to be refined.

285 To this purpose we search for a minimizer of the energy  $\Phi_\varepsilon(U, w)$  via solving equations  
 286 (14) with initial data  $U_0$  given by  $\nabla f$ . So that we obtain a vector field  $U$  whose divergence  
 287 is relevant only on the set  $P$  and a function  $w$  whose zeros are given by the set  $P$ .

### 288 6.1 Discretization

The image is an array of size  $N^2$ . We endowed the space  $R^{N \times N}$  with the standard scalar product and standard norm. The gradient  $\nabla I \in (R^{N \times N}) \times (R^{N \times N})$  is given by:

$$(\nabla I)_{i,j} = ((\nabla I)_{i,j}^1, (\nabla I)_{i,j}^2)$$

where

$$(\nabla I)_{i,j}^1 = \begin{cases} I_{i+1,j} - I_{i,j} & \text{if } i < N \\ 0 & \text{if } i = N, \end{cases}$$

$$(\nabla I)_{i,j}^2 = \begin{cases} I_{i,j+1} - I_{i,j} & \text{if } j < N \\ 0 & \text{if } j = 0. \end{cases}$$

289 We also introduce the discrete version of the divergence operator simply defined as the  
 290 adjoint operator of the gradient:  $\text{div} = -\nabla^*$ . More in details if  $v \in (R^{N \times N}) \times (R^{N \times N})$ , we  
 291 have

$$(\operatorname{div} v)_{i,j} = \begin{cases} v_{i,j}^1 + v_{i,j}^2 & \text{if } i, j = 1 \\ v_{i,j}^1 + v_{i,j}^2 - v_{i-1,j}^2 & \text{if } i = 1, 1 < j < N \\ v_{i,j}^1 - v_{i-1,j}^1 + v_{i,j}^2 - v_{i-1,j}^2 & \text{if } 1 < i < N, 1 < j < N \\ -v_{i-1,j}^1 + v_{i,j}^2 - v_{i-1,j}^2 & \text{if } i = N, 1 < j < N \\ v_{i,j}^1 - v_{i-1,j}^1 + v_{i,j}^2 & \text{if } 1 < i < N, j = 1 \\ v_{i,j}^1 - v_{i-1,j}^1 - v_{i-1,j}^2 & \text{if } 1 < i < N, j = N \\ -(v_{i-1,j}^1 + v_{i-1,j}^2) & \text{if } i, j = N. \end{cases}$$

292 Then we can define the discrete version of the Laplacian operator as  $\Delta I = \operatorname{div}(\nabla I)$ .

## 293 6.2 Discretization in time

We simply replace  $\frac{\partial U}{\partial t}$  and  $\frac{\partial w}{\partial t}$  by  $\frac{U_{i,j}^{n+1} - U_{i,j}^n}{\delta t}$  and  $\frac{w_{i,j}^{n+1} - w_{i,j}^n}{\delta t}$  respectively. Then we write system (14) in the form (for simplicity we omit the dependence on  $\varepsilon$ )

$$\begin{cases} U_1^{n+1} = -\delta t \Phi_{U_1}(U_n, w_n) \\ U_2^{n+1} = -\delta t \Phi_{U_2}(U_n, w_n) \\ w^{n+1} = -\delta t \Phi_w(U_n, w_n). \end{cases}$$

294 We initialize our algorithm with  $U(0) = \nabla f$ , where  $f$  is the solution of problem (15). To do  
295 this, we need to solve a Dirichlet problem with data measure  $I$ , therefore we regularize the  
296 image by convolution with a Gaussian kernel  $G_\sigma$  with very small  $\sigma$  and then we solve, by  
297 classical finite differences method, the problem:

$$\begin{cases} \Delta f = I_\sigma & \text{on } \Omega \\ f = 0 & \partial\Omega, \end{cases} \quad (16)$$

298 where  $I_\sigma = I * G_\sigma$ .

299 To initialize our algorithm, we need of an initial guess on  $w$ . So we choose  $w(0) = 1$ .

## 300 7 Computer examples

### 301 7.1 Parameter settings

302 Before running our algorithm all the parameters have to be fixed. The most important  
 303 are  $\varepsilon$ ,  $\beta_\varepsilon$  and  $\mu_\varepsilon$ , which govern the set  $D$  approximating points we want to detect. Those  
 304 parameters are related by the conditions  $\lim_{\varepsilon \rightarrow 0} \frac{\varepsilon |\log(\varepsilon)|}{\beta_\varepsilon} = 0$ ,  $\lim_{\varepsilon \rightarrow 0} \frac{\beta_\varepsilon}{\mu_\varepsilon} = 0$ . Furthermore, since  
 305 the mesh grid size is 1 and  $\beta_\varepsilon$  gives the radius of a ball centered in the singular point we  
 306 want to detect, from a discrete point of view the smallest value we can take is  $\frac{\sqrt{2}}{2}$ . Then we  
 307 use the values 0.1 for  $\varepsilon$ , 0.7 for  $\beta_\varepsilon$ , and 0.8 for  $\mu_\varepsilon$ . As exponent  $p$  of the discrepancy term  
 308 we always take  $p = 1.5$

309 Concerning the parameter  $\lambda$  we mainly used the value  $\lambda = 0.1$ , in order to force the  
 310 algorithm to regularize as much as possible the initial data  $U_0$ .

311 Since we deal with small values of  $\varepsilon$ , in order to have some stability, we must take a  
 312 small discretization time step. Practically we mainly used the value  $\delta t = 1 \times 10^{-6}$ .

313 Concerning the stopping criterion we iterate the algorithm until  $\max \left\{ \frac{\|U_1^{n+1} - U_1^n\|_1}{\|U_1^n\|_1}, \frac{\|U_2^{n+1} - U_2^n\|_1}{\|U_2^n\|_1}, \frac{\|w^{n+1} - w^n\|_1}{\|w^n\|_1} \right\}$   
 314  $\leq 1 \times 10^{-2}$ .

315 In all the computer examples the points are detected by means of the function  $w_\varepsilon$ . We  
 316 display the level-set  $\{w_\varepsilon \simeq 0\}$ .

### 317 7.2 Commentaries

318 The figure 1 shows how resistant to the noise our model is. When the noise is larger the  
 319 parameter  $\varepsilon$  must be as close as possible to the ideal value 0. Besides it is possible to see  
 320 that for small values of  $\varepsilon$  our detection is very fine according to the continuous setting. More  
 321 in details in the first row we display the initial image obtained by adding a Gaussian noise  
 322 to a binary image of five points. The second row shows the behavior of  $w_\varepsilon$  for small values  
 323 of  $\varepsilon$  and  $\beta_\varepsilon$ .

324 Looking at the histograms of the gray level of  $I$  and  $w_\varepsilon$ , one can see that it is easier  
 325 fixing a threshold value starting from the function  $w_\varepsilon$  than from the initial image  $I$ . In the  
 326 last row we display the set  $\{w_\varepsilon \simeq 0\}$  obtained by plotting the set  $\{w_\varepsilon \leq \alpha\}$  with threshold  
 327 value  $\alpha = 0.5$ .

328 In figure 2 we test our algorithm on curves and points at the same time. In the first row  
 329 we have a sequence of points and a curve with boundary inside  $\Omega$ . In the second row we  
 330 display the function  $w_\varepsilon$  and the level set  $\{w_\varepsilon \simeq 0\}$  once again obtained by fixing a threshold  
 331 value  $\alpha = 0.5$ . The result is that, as desired, our algorithm is capable of eliminating the  
 332 curve from the initial image. According to the continuous setting when  $\varepsilon$  takes values close  
 333 to 0 the approximating energy (13) behaves similarly to the limit energy (1), so that the  
 334 presence of the curve is penalized in the minimization process. Then the set  $\{w_\varepsilon \simeq 0\}$   
 335 contains nothing else but points.

336 Finally in figure (a),(b),(c) and (d) we deal with a biological image. Our task is catch-  
 337 ing the finest structure present in the image. In figure (d) the isolated points are quite

338 well detected, while the branches the cellule are not. Nevertheless due to the small time  
 339 discretization step the computation time is quite large. To test the image in (a) of size  
 340  $500 \times 500$ , our algorithm takes 100 iterations and about 7mm. Certainly the algorithm can  
 341 be accelerated by using more sophisticated techniques such as multigrid methods. Such a  
 faster algorithm is the subject of our current investigation.

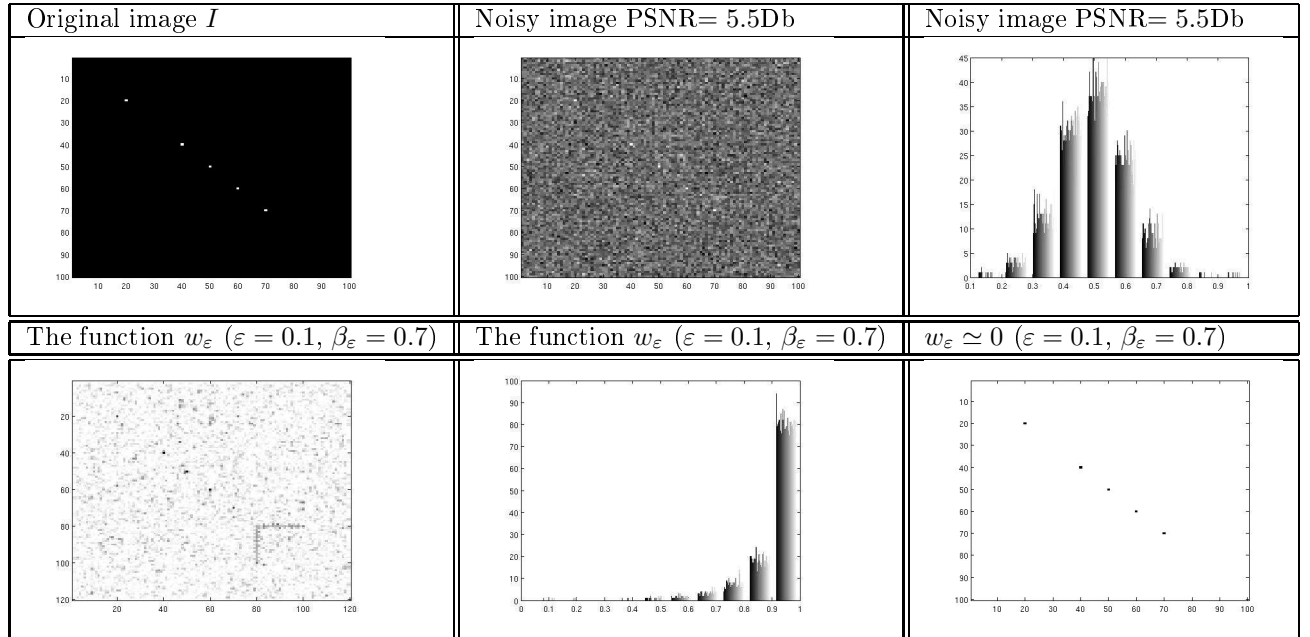


Figure 1: *Synthetic image: we test our algorithm on noisy images. When the parameters  $\varepsilon$  and  $\beta_\varepsilon$  are small as much as possible the detection is finer. The detection is refined by fixing a threshold value  $\alpha$  for the function  $w_\varepsilon$*

342

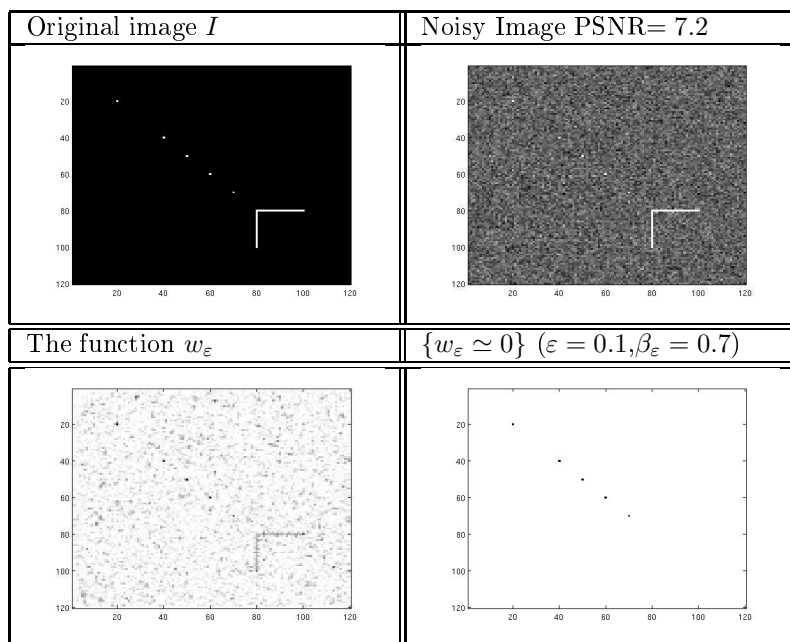
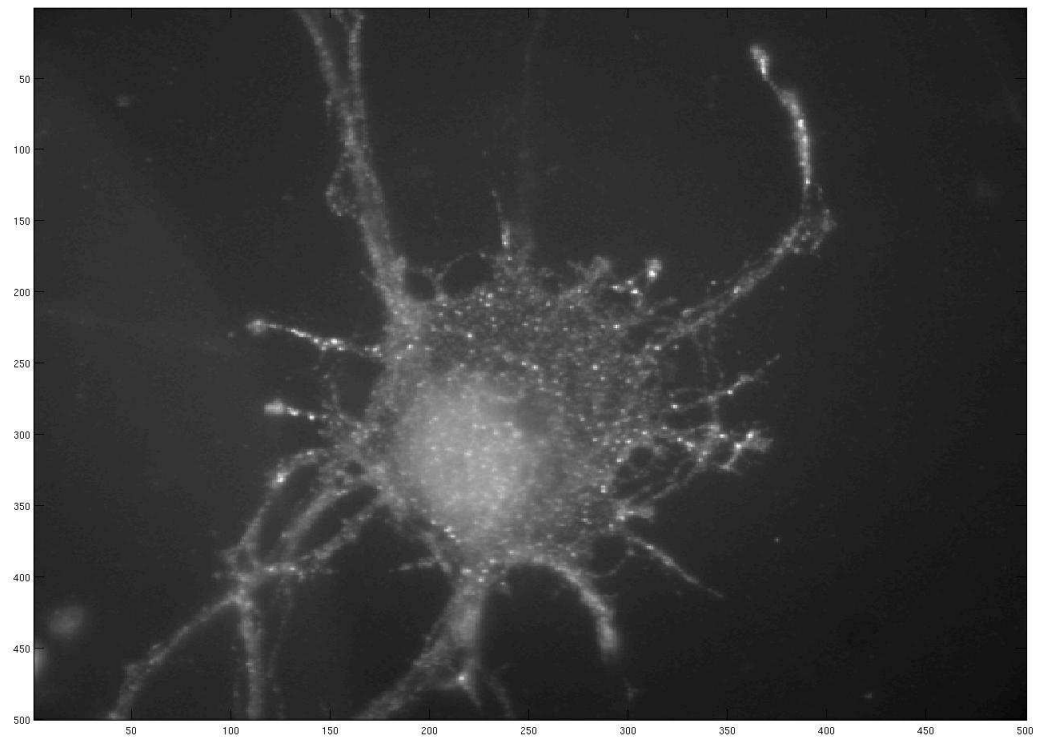
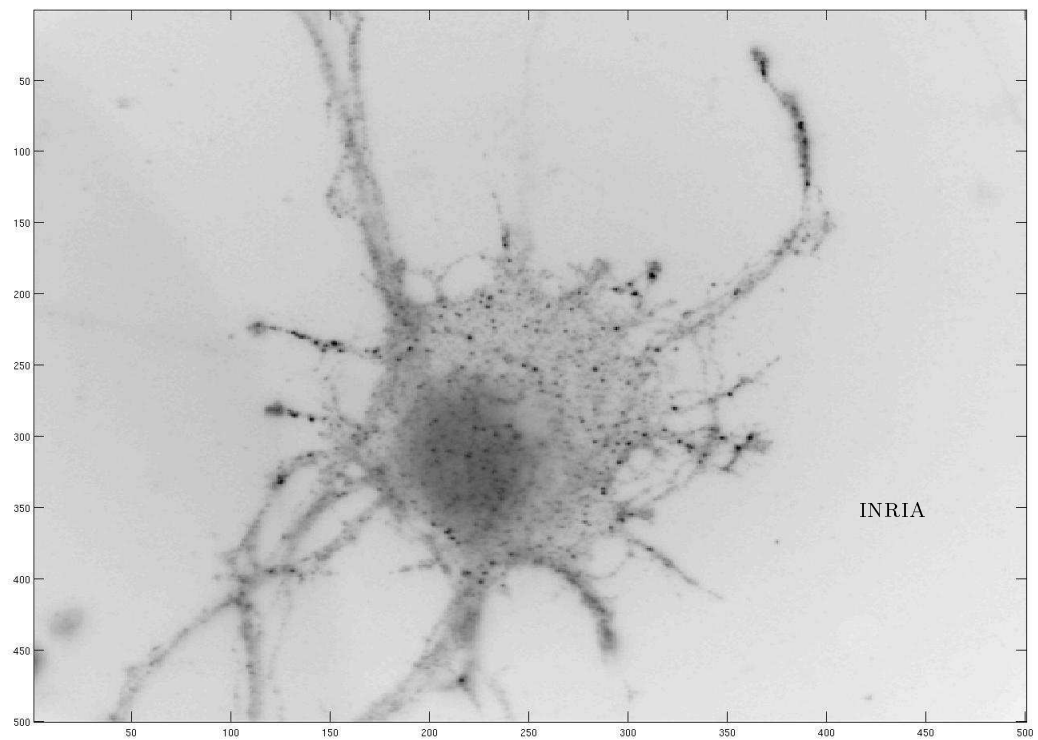


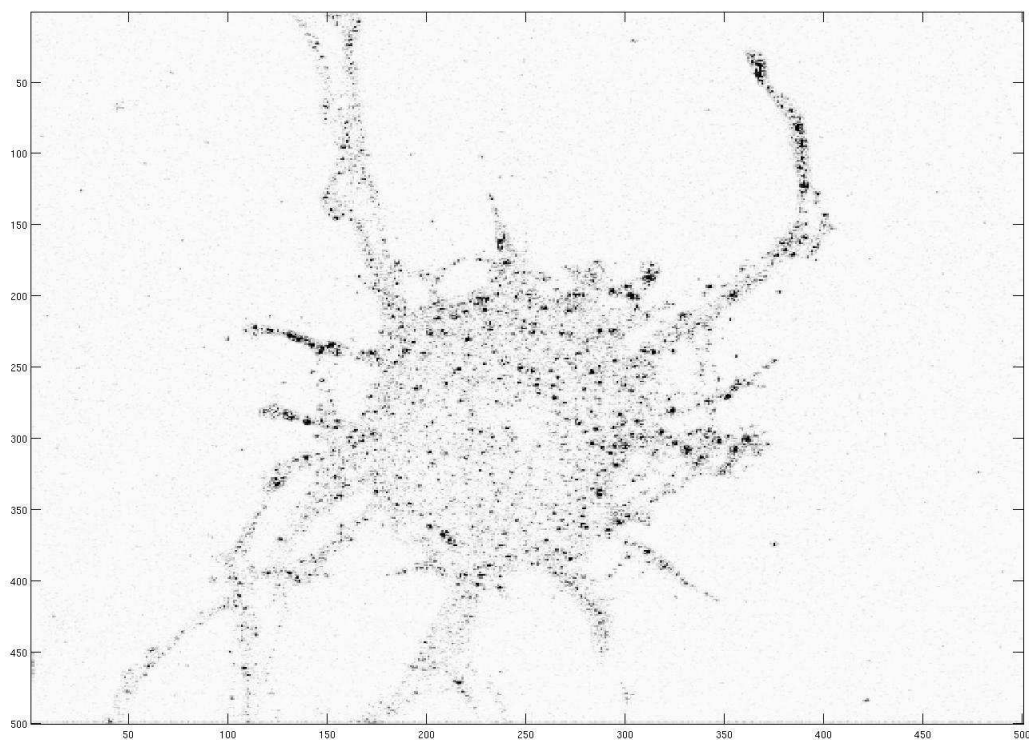
Figure 2: Synthetic image: curve points and noise are present in the initial image. As expected our method is capable of removing the curve from the image.



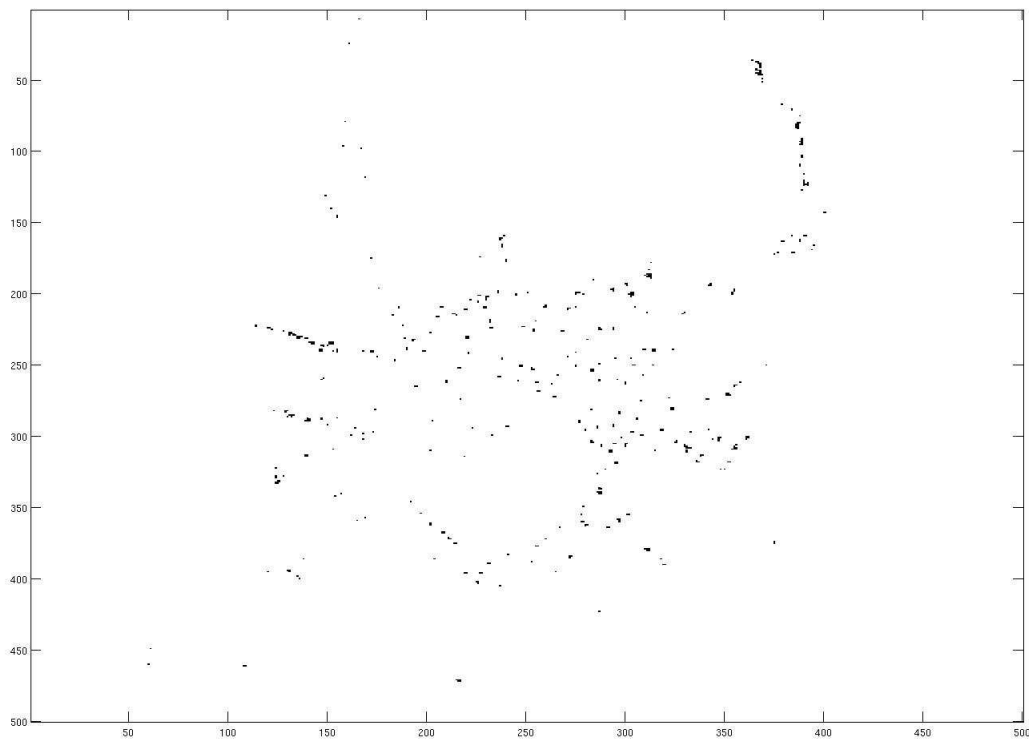


(a) Original Image

(b) Superposition of the original image with the set  $\{w_\varepsilon \approx 0\}$  ( $\varepsilon = 0.1, \beta_\varepsilon = 0.7$ )



(c) The function  $w_\varepsilon$  ( $\varepsilon = 0.1$ ,  $\beta_\varepsilon = 0.7$ )



RR n° 7038

(d) the set  $\{w_\varepsilon \simeq 0\}$  ( $\varepsilon = 0.1$ ,  $\beta_\varepsilon = 0.7$ )

## 343 8 Conclusion

344 In this work, a new variational method for spot detection in biological images has been  
345 proposed and tested. We emphasize that, according to our knowledge, this is the first  
346 method which makes possible isolating the spots from a filament in the observed image.  
347 Moreover it also permits in a noisy image to fix a threshold value in a simple and direct way.  
348 Moreover we believe that a suitable generalization of this method for the detection of spots  
349 and even filaments in 3-D biological images can be provided. This is a subject of our current  
350 investigation. Certainly there are many rooms for improvement both from a theoretical and  
351 numerical point of view such as a deep investigation of the  $\Gamma$ -convergence approximation, as  
352 a well as a significant acceleration of the algorithm.

353 **References**

- 354 [1] L.Ambrosio, N.Fusco, D.Pallara. *Functions of bounded variation and free discontinuity*  
355 *problems*. Oxford University Press (2000).
- 356 [2] L.Ambrosio, V.M.Tortorelli. *Approximation of functionals depending on jumps by elliptic*  
357 *functionals via  $\Gamma$ -convergence*. *Communic. Pure Appl. Math* **43** (1990), 999-1036.
- 358 [3] L.Ambrosio, V.M.Tortorelli. *Approximation of functionals depending on jumps by*  
359 *quadratic, elliptic functionals via  $\Gamma$ -convergence*. *Boll.Un. Mat. Ital.* 6-B(1992), 105-123.
- 360 [4] G.Anzellotti *Pairings between measures and bounded functions and compensated com-*  
361 *pactness*. *Ann. Mat. Pura Appl.* **135** (1983), 293-318.
- 362 [5] G.Aubert, J. Aujol, L.Blanc-Feraud *Detecting Codimension-Two Objects in an image*  
363 *with Ginzburg-Landau Models*. *International Journal of Computer Vision* **65** (2005), 29-  
364 42.
- 365 [6] G.Aubert, D.Graziani *Variational approximation for detecting points like-target problem*  
366 *in 2-D biological images* submitted to ESAIM: COCV. Preprint available on [http://www-](http://www-sop.inria.fr/en/publications.php)  
367 [sop.inria.fr/en/publications.php](http://www-sop.inria.fr/en/publications.php).
- 368 [7] F. Bethuel, H. Brezis and F. Hélein *Ginzburg-Landau Vortices*. Birkäuser, Boston (1994).
- 369 [8] A.Braides.  *$\Gamma$ -convergence for beginners*. Oxford University Press, New york (2000).
- 370 [9] A.Braides, A.Malchiodi *Curvature Theory of Boundary phases: the two dimensional*  
371 *case*. *Interfaces Free. Bound.* **4** (2002), 345-370.
- 372 [10] A.Braides, R.March. *Approximation by  $\Gamma$ -convergence of a curvature-depending func-*  
373 *tional in Visual Reconstruction* *Comm. Pure Appl. Math.* **59** (2006), 71-121.
- 374 [11] G.Dal Maso. *Introduction to  $\Gamma$ -convergence*. Birkhäuser, Boston(1993).
- 375 [12] E.De Giorgi *Some Remarks on  $\Gamma$ -convergence and least square methods, in* *Com-*  
376 *posite Media and Homogenization Theory* (G. Dal Maso and G.F.Dell'Antonio eds.),  
377 Birkhauser, Boston, 1991, 135-142.
- 378 [13] E.De Giorgi, T.Franzoni. *Su un tipo di convergenza variazionale*. *Atti Accad. Naz. Lincei*  
379 *Rend. Cl. Sci. Mat. Natur.* **58** (1975), 842-850.
- 380 [14] E.De Giorgi, T.Franzoni. *Su un tipo di convergenza variazionale*. *Rend. Sem. Mat.*  
381 *Brescia* **3** (1979), 63-101.
- 382 [15] L.Modica, S.Mortola. *Un esempio di  $\Gamma$ -convergenza*. *Boll.Un. Mat. Ital.* 14-B(1977),  
383 285 – 299.

- 
- 384 [16] L.Modica. *The gradient theory of phase transitions and the minimal interface criterion.*  
385 Arch. Rational Mech. Anal. **98** (1987), 123-142.
- 386 [17] M.Morel, Solimini *Variational models in image segmentation*, Birkäuser, 1994.
- 387 [18] M.Röger, R.Shätzle. *On a modified conjecture of De Giorgi.* Math. Zeitschrift. **254**  
388 (2006), 675-714
- 389 [19] G.Stampacchia *Le problème de Dirichlet pour les equations elliptiques du seconde ordre*  
390 *à coefficients discontinuous.* Ann. Inst. Fourier (Grenoble), **15** (1965), 180-258.
- 391 [20] A.Witkin, D.Terzopoulos, M.Kass. *Signal mathcing trough scale space* International  
392 Journal of Computer Vision 1 **2** (1987), 133-144.



---

Unité de recherche INRIA Sophia Antipolis  
2004, route des Lucioles - BP 93 - 06902 Sophia Antipolis Cedex (France)

Unité de recherche INRIA Futurs : Parc Club Orsay Université - ZAC des Vignes  
4, rue Jacques Monod - 91893 ORSAY Cedex (France)

Unité de recherche INRIA Lorraine : LORIA, Technopôle de Nancy-Brabois - Campus scientifique  
615, rue du Jardin Botanique - BP 101 - 54602 Villers-lès-Nancy Cedex (France)

Unité de recherche INRIA Rennes : IRISA, Campus universitaire de Beaulieu - 35042 Rennes Cedex (France)

Unité de recherche INRIA Rhône-Alpes : 655, avenue de l'Europe - 38334 Montbonnot Saint-Ismier (France)

Unité de recherche INRIA Rocquencourt : Domaine de Voluceau - Rocquencourt - BP 105 - 78153 Le Chesnay Cedex (France)

---

Éditeur  
INRIA - Domaine de Voluceau - Rocquencourt, BP 105 - 78153 Le Chesnay Cedex (France)  
<http://www.inria.fr>  
ISSN 0249-6399